HHS Public Access

Author manuscript

Mol Imaging Biol. Author manuscript; available in PMC 2017 January 18.

Published in final edited form as:

Mol Imaging Biol. 2011 February ; 13(1): 112–120. doi:10.1007/s11307-010-0302-4.

Specific Targeting of Human Integrin $\alpha_v\beta_3$ with ^{111}In-Labeled Abegrin™ in Nude Mouse Models

Zhaofei Liu[1], **Bing Jia**[1], **Huiyun Zhao**[1], **Xiaoyuan Chen**[2,3], and **Fan Wang**[1]

[1]Medical Isotopes Research Center and Department of Radiation Medicine, School of Basic Medical Sciences, Peking University, 38 Xueyuan Road, Beijing 100191, China

[2]Molecular Imaging Program at Stanford (MIPS), Department of Radiology, Biophysics, and Bio-X Program, Stanford University School of Medicine, Stanford, CA 94305, USA

[3]Laboratory of Molecular Imaging and Nanomedicine (LOMIN), National Institute of Biomedical Imaging and Bioengineering (NIBIB), National Institutes of Health (NIH), Bethesda, MD 20892, USA

Abstract

Purpose—The cell adhesion molecule integrin $\alpha_v\beta_3$ is an important player in the process of tumor angiogenesis and metastasis. Abegrin™, a fully humanized anti-integrin $\alpha_v\beta_3$ monoclonal antibody, was currently in clinical trials for cancer therapy. Herein, we labeled Abegrin™ with ^{111}In, evaluated the *in vitro* and *in vivo* characteristics, and investigated whether the expression of integrin $\alpha_v\beta_3$ in tumors could be imaged with ^{111}In-labeled Abegrin™.

Methods—The binding affinity and specificity of Abegrin™ was analyzed using U87MG glioblastoma cells. Abegrin™ was coupled with 1,4,7,10-tetraazadodecane-N,N,N',N"-tetraacetic acid (DOTA) for ^{111}In radiolabeling. γ Imaging of ^{111}In-DOTA–Abegrin™ was carried out in nude mice bearing both integrin $\alpha_v\beta_3$-positive U87MG and integrin $\alpha_v\beta_3$-negative HT-29 tumors. Biodistribution and blocking studies of ^{111}In-DOTA–Abegrin™ were investigated in U87MG tumor-bearing nude mice.

Results—Abegrin™ exhibited high-binding affinity to human integrin $\alpha_v\beta_3$ expressed on U87MG cells (K_d of 0.35±0.06 nM). The antibody retained antigen-binding affinity/specificity after DOTA conjugation. γ Imaging showed that the tumor uptake of ^{111}In-DOTA–Abegrin™ in integrin $\alpha_v\beta_3$-positive U87MG tumors was much higher than that in integrin $\alpha_v\beta_3$-negative HT-29 tumors. In the HT-29 tumors, Abegrin™ was mainly nonspecifically accumulated around the blood vessels, while in the U87MG tumors, besides the nonspecific tumor retention, Abegrin™ also specifically bound the human integrin $\alpha_v\beta_3$ expressed on the tumor cells. Biodistribution and blocking studies exhibited that the U87MG tumor uptake of ^{111}In-DOTA–Abegrin™ decreased from 14.12±0.44 to 6.93±0.94 percentage of injected dose per gram of tissue after coinjection of excess dose of cold Abegrin™, which confirmed the *in vivo* integrin $\alpha_v\beta_3$ binding specificity of ^{111}In-DOTA–Abegrin™.

Correspondence to: Fan Wang; wangfan@bjmu.edu.cn.

Conclusions—Abegrin™ showed specific binding to human integrin $\alpha_v\beta_3$ expressed on the tumor cells. ^{111}In-DOTA–Abegrin™ can specifically target the human integrin $\alpha_v\beta_3$ expression in the nude mouse model. ^{111}In-DOTA–Abegrin™ has a potential for clinical translation as an agent for integrin $\alpha_v\beta_3$-positive tumor imaging, evaluating tumor angiogenic status and monitoring the therapeutic efficacy of Abegrin™-based cancer therapy.

Keywords

Tumor; Integrin $\alpha_v\beta_3$; ^{111}In; Abegrin™; Imaging

Introduction

Integrins are a family of cell surface adhesion receptors consisting of two heterodimeric subunits (α and β), with function to promote invasion and support survival, as well as to regulate cell adhesion [1, 2]. As an important member of this family, integrin $\alpha_v\beta_3$ is generally not found in normal tissues but is highly expressed on activated endothelial cells during tumor angiogenesis, as well as some tumor cells, such as late-stage glioblastomas, breast and prostate tumors, malignant melanomas, and ovarian carcinomas [3–5]. Increased expression of integrin $\alpha_v\beta_3$ is closely associated with tumor biological activities, including angiogenesis, cell adhesion, invasion, and metastasis [6, 7]. Inhibition of integrin $\alpha_v\beta_3$ function using blocking monoclonal antibodies, peptide antagonists, and small peptide mimetics matrix has been shown to be a promising strategy for antiangiogenic cancer therapy [8–10].

In the past decade, radiolabeled arginine-glycine-aspartic acid (RGD) peptides and analogs have been wildly investigated for noninvasive imaging of tumor integrin $\alpha_v\beta_3$ expression in both animal models and clinical trials [11–14], based on the recognition between RGD and integrin $\alpha_v\beta_3$. In addition to RGD peptides, anti-integrin $\alpha_v\beta_3$ antibodies were also generated and evaluated as integrin $\alpha_v\beta_3$-targeting vehicles. Abegrin™, also known as MEDI-522 or Vitaxin™, is a humanized monoclonal antibody against human integrin $\alpha_v\beta_3$, which is currently in clinical trials for the treatment of stage IV metastatic melanoma and androgen-independent prostate cancer [15, 16]. Unlike other antibodies, Abegrin™ recognizes the integrin α_v and β_3 subunits as one entity [16, 17], which makes it much more specific for integrin $\alpha_v\beta_3$ [18]. In a recent clinical study, Abegrin™ was well tolerated with no evidence of immunogenicity in patients with advanced solid tumors, which guaranteed its further clinical investigation [19].

Radiolabeled monoclonal antibodies have been developed for both diagnosis and therapy of tumors. We recently reported the radioimmunotherapy of ^{90}Y-labeled Abegrin™ in the glioblastoma tumor model [8]. The ^{90}Y-DOTA–Abegrin™ showed promising therapeutic efficacy in the integrin $\alpha_v\beta_3$-positive tumor models as monitored by 2-deoxy-2-[F-18]fluoro-D-glucose (FDG) and 3’-[F-18] fluoro-3’-deoxythymidine (FLT)-based micro-PET imaging. ^{99m}Tc-labeled hLM609-I, the earlier version of Abegrin™, was previously tested for the *in vivo* imaging of tumor vasculature. However, the imaging was unsuccessful due to the instability of ^{99m}Tc labeling [20]. Cai *et al.* recently evaluated the *in vitro* and *in vivo* characterizations of ^{64}Cu ($t_{1/2}$ = 12.7 h; β^+, 17%; β^- , 39%)-labeled Abegrin™ in nude

mouse tumor models. The probe showed high and specific tumor uptake in integrin $\alpha_v\beta_3$-positive tumors, which makes the ^{64}Cu-labeled tracer promising for evaluating the pharmacokinetics, tumor targeting efficacy, and dose optimization of Abegrin™ [21]. Comparing with ^{64}Cu, ^{111}In ($t_{1/2}$ = 2.8 days; γ, 173 keV, 89%; 247 keV, 94%) possesses more suitable half-life for antibody-based tumor imaging, which allows a long-term observation of the *in vivo* behaviors and clinical imaging with a gamma camera or single photon emission computed tomography (SPECT). Nowadays, a series of ^{111}In-labeled antibodies have been used in clinical trials for tumor imaging and monitoring the therapeutic efficacy of anticancer drugs [22–25]. In this study, we labeled Abegrin™ with ^{111}In using 1,4,7,10-tetraazadodecane-*N,N′,N″,N‴*-tetraacetic acid (DOTA) as the chelator, tested the *in vitro* immunoreactivity and affinity, and investigated the *in vivo* tumor targeting properties in integrin $\alpha_v\beta_3$-positive U87MG tumors and also in integrin $\alpha_v\beta_3$-negative HT-29 tumors.

Materials and Methods

Materials and Reagents

The humanized anti-integrin $\alpha_v\beta_3$ monoclonal antibody (mAb) Abegrin™ (MEDI-522 or Vitaxin™) was obtained from MedImmune, Inc. (Gaithersburg, MD). Macrocyclic chelating agent DOTA was purchased from Macrocyclics, Inc. (Dallas, TX). 1-Ethyl-3-[3-(dimethylamino)-propyl] carbodiimide (EDC) and N-hydroxysulfonosuccinimide (SNHS) were purchased from Aldrich (St. Louis, MO). $^{111}InCl_3$ was obtained from Perkin-Elmer Life and Analytical Sciences (North Billarica, MA). PD-10 desalting columns were purchased from GE Healthcare (Piscataway, NJ). All water and buffers used for DOTA conjugation and radiolabeling were passed through a Chelex 100 (Sigma-Aldrich, St. Louis, MO) column to minimize the trace metal contaminants.

Cell Culture and Animal Models

U87MG human glioblastoma cells and HT-29 human colon cancer cells were obtained from American Type Culture Collection (Manassas, VA). U87MG cells were cultured in low glucose Dulbecco's Modified Eagle's Medium (DMEM) [21], and HT-29 cells were cultured in high-glucose DMEM culture medium [26]. Both cell lines were cultured in medium supplemented with 10% (v/v) fetal bovine serum at 37°C in a humidified atmosphere with 5% CO_2. Female BALB/c nude mice (4~5 weeks of age) were purchased from the Department of Experimental Animal, Peking University Health Science Center. All animal experiments were performed in accordance with guidelines of Peking University Health Science Center Animal Care Committee (Institutional Animal Care and Use Committee at Peking University). U87MG tumor model was established by subcutaneous injection of 2×10^6 U87MG tumor cells into the right upper flanks of nude mice. When the tumor volume reached 200~300 mm^3 (3~4 weeks after inoculation), the U87MG tumor-bearing nude mice were used for biodistribution studies. To establish another tumor model bearing both U87MG and HT-29 tumor xenografts, the U87MG cells (2×10^6) were first inoculated subcutaneously into the right upper flanks of mice. After about 15 days, HT-29 cells (5×10^6) were inoculated subcutaneously into left upper flanks of the same nude mice. In this condition, the two tumors reached a similar volume (200~300 mm^3) after another 13 days, and then they were used for *in vivo* studies.

Saturation Binding Assay

The binding affinity of mAb Abegrin™ for integrin $\alpha_v\beta_3$ and the available binding sites per U87MG cell were measured by saturation binding assay [27]. Briefly, ^{125}I-Abegrin™ was generated by incubating Abegrin™ (50 μg) with Na^{125}I (37 MBq) in a vial coated with Iodogen (Sigma-Aldrich, St. Louis, MO) and then purified by a PD-10 column using a previously described method [28]. U87MG cells were seeded in a Filter multiscreen DV plate (96-well; pore size, 0.65 μm; Millipore) and then incubated with increasing concentrations of ^{125}I-Abegrin™ (from 0.033 to 16.67 nM) in binding buffer (20 mM Tris, pH 7.4, 150 mM NaCl, 2 mM $CaCl_2$, 1 mM $MgCl_2$, 1 mM $MnCl_2$, and 0.1% BSA). The total volume was adjusted to 200 μL using binding buffer. For each concentration, nonspecific binding was determined in the presence of an excess (>100-fold) unlabeled mAb Abegrin™. After 4 h of incubation at 4°C, the plate was filtered through a multiscreen vacuum manifold and washed five times with cold phosphate-buffered saline (PBS). The hydrophilic polyvinylidenedifluoride (PVDF) filters were collected, and the radioactivity was determined using a NaI (Tl) γ-counter (Wallac 1470-002, Perkin-Elmer, Finland). A saturation binding curve and Scatchard transformation were obtained by a nonlinear regression analysis, and the dissociation constant (K_d) value of ^{125}I-Abegrin™ and the binding sites per U87MG cell were determined using GraphPad Prism 4.0 (GraphPad Software, San Diego, CA). Each data point represents the average value from triplicate wells.

DOTA Conjugation and ^{111}In Radiolabeling

Abegrin™ was conjugated with DOTA as previously described [21]. Briefly, DOTA was activated by EDC and SNHS at pH 5.5 for 30 min at 4°C with a molar ratio of 10:5:4 (DOTA/EDC/SNHS). The DOTA–*N*-hydroxysulfosuccinimidyl (OSSu) was then added to Abegrin™ at the molar ratio of DOTA–OSSu/Abegrin™=200:1 in the bicarbonate buffer (pH = 9.0). After incubating overnight at 4°C, the DOTA–Abegrin™ conjugates were then purified by PD-10 column and concentrated by Centricon filter (Millipore, Bedford, MA), and the final concentration was determined using a micro-BCA protein assay kit (Pierce Biotechnology).

For ^{111}In radiolabeling, 74 MBq of $^{111}InCl_3$ (2 mCi) was diluted in 300 μL of 0.2 M sodium acetate buffer (pH 5.5) and added to 50 μg of DOTA–Abegrin™. The reaction mixture was incubated for 1 h at 39°C with constant shaking. ^{111}In-DOTA–Abegrin™ was then purified by PD-10 column using PBS as the mobile phase.

Immunoreactivity and Specificity

The immunoreactivity of DOTA–Abegrin™ and intact Abegrin™ to integrin $\alpha_v\beta_3$ was evaluated by whole-cell displacement assay [29]. The U87MG cells were incubated with ^{125}I-Abegrin in the presence of increasing concentrations of Abegrin™ or DOTA–Abegrin™ in a 96-well filter plate. After 2 h of reaction at 4°C, the plates were washed, then the PVDF filters were collected, and measured in a γ-counter as described above. The best-fit 50% inhibitory concentration (IC_{50}) values were calculated by fitting the data with nonlinear regression using Graph Pad Prism 4.0 (GraphPad Software, Inc.). Experiments were performed twice with triplicate samples.

The integrin binding specificity of ^{111}In-DOTA–Abegrin™ was tested using U87MG cells. U87MG cells were seeded in six-well plates and incubated overnight at 37°C to allow adherence. After washing with PBS, 250 μL of the ^{111}In-DOTA–Abegrin solution (10 ng/mL in culture medium) was added to the wells of the plate with or without an excess amount of cold Abegrin™ (5 μg/mL). The cells were then incubated at 4°C for 2 h, after which the cells were washed and then collected by trypsinizing with 0.25% trypsin solution. The cell-associated radioactivity was measured in γ-counter. Results were expressed as percentage of the total added dose per million cells (%AD/10^6 cells). Experiments were carried out twice with the triplicate samples.

Immunofluorescent Staining

The immunofluorescent staining of tumor cells were performed as we previously described [21, 30]. Briefly, U87MG or HT-29 cells were incubated with Abegrin™ (2 μg/mL) for 1 h at room temperature. After washing, the cells were visualized with Cy3-labeled donkey antihuman IgG (1:500) under the microscope (Carl Zeiss Axiovert 200 M, Carl Zeiss, Thornwood, NY).

U87MG and HT-29 tumor tissue sections (5 μm-thick) were cut from the frozen blocks, mounted on coated slides, fixed in acetone for 10 min, and allowed to dry in the air for 30 min. The sections were blocked with 10% donkey serum for 1 h at room temperature. For murine integrin $\alpha_v\beta_3$ and human integrin $\alpha_v\beta_3$ double staining, the sections were incubated with hamster antimouse integrin β_3 (1:100; BD Biosciences, San Jose, CA) and Abegrin™ (10 μg/mL) for 1 h at room temperature. After incubating with Cy3-conjugated donkey antihamster secondary antibody (1:200; Jackson ImmunoResearch Laboratories) and fluorescein isothiocyanate (FITC)-conjugated donkey antihuman secondary antibody (1:200), the tumor sections were examined under the microscope (Carl Zeiss Axiovert 200 M, Thornwood, NY).

Integrin $\alpha_v\beta_3$ Expression on Tumor Cells

The U87MG and HT-29 cells grown in 24-well plates (1×10^5/well) were incubated with ~80,000 cpm of ^{125}I-Abegrin™. For each cell line, nonspecific binding was determined in the presence of an excess (>100-fold) unlabeled Abegrin™. The total volume was adjusted to 250 μL with 1% bovine serum albumin (in PBS). After incubating for 3 h at 4°C, the cells in the plate were washed gently with PBS for three times and then solubilized with 2 M NaOH. The cell-associated activity was measured in a γ-counter. Experiments were carried out twice with triplicate wells. Results were expressed as percentage of added dose per million cells (%AD/10^6 cells).

Planar γ Imaging

Each nude mouse bearing both U87MG and HT-29 tumor xenografts was injected with ~11.1 MBq (300 μCi) of ^{111}In-DOTA–Abegrin™ via tail vein ($n = 3$). Animals were anesthetized with intraperitoneal injection of sodium pentobarbital at a dose of 45.0 mg/kg and then placed prone on a two-headed camera (SIEMENS, E. CAM) equipped with a parallel-hole, middle-energy, and high-resolution collimator. Posterior images were acquired

at 2, 24, 48, and 120 h postinjection (p.i.) and stored digitally in a 128×128 matrix. The acquisition count limits were set at 200 K.

In Vivo Microdistribution of FITC–Abegrini™ in Tumors

Abegrin™ was conjugated with FITC–NHS (Pierce, Rockford, IL, USA) according to the standard protocol and purified with PD-10 column. The *F/P* ratio (fluorochrome/protein ratio, i.e., FITC-to-Abegrin™ ratio) of FITC–Abegrin™ after purification was measured based on UV absorbance using the following equation: $F/P = 3{:}1 \times A_{495}/[A_{280} - 0{:}31 \times A_{495}]$. The *F/P* ratio was calculated to be 4.70. The FITC–Abegrin™ was passed through a 0.22-μm Millipore filter and stored at 4°C. A nude mouse bearing both the U87MG and HT-29 tumor xenografts was injected with 200 μg FITC–Abegrin™ via tail vein. At 24 h postinjection, the mouse was anesthetized, sacrificed, and perfused through the heart with 25 mL PBS. The tumors were removed, frozen, and cut into 5-μm-thick slices. The slices were stained with rat antimouse CD31 antibody (1:100; BD Bio-sciences) and then visualized with Cy3-conjugated donkey antirat secondary antibody (1:200; Jackson Immuno-Research Laboratories, Inc.).

Biodistribution and Blocking Studies

Female nude mice bearing U87MG xenografts were injected with 0.74 MBq (20 μCi) of ^{111}In-DOTA–Abegrin™ via tail vein to evaluate the distribution of the tracer in the major organs of mice. At 4, 24, 72, 120, and 168 h p.i., mice were sacrificed. Blood, tumor, major organs, and tissues were collected, wet-weighted, and measured using a γ counter. The results were presented as percentage of injected dose per gram of tissue (%ID/g). Values are expressed as means±SD for a group of four animals (n=4 per group). A blocking study was also performed in a group of four mice by coinjecting ^{111}In-DOTA–Abegrin™ with 400 μg unlabeled Abegrin™. At 24 h p.i., all four animals were sacrificed for determination of organ biodistribution as described above.

Results

Saturation Binding Assay

The saturation binding curve and the Scatchard transformation of ^{125}I-Abegrin™ on U87MG cells are shown in Fig. 1a, b. The K_d value for ^{125}I-Abegrin™ was determined to be 0.35±0.06 nM, and the maximum number of binding sites (B_{max}) was 2.5×10^5 receptors per U87MG cell, indicating the high affinity of Abegrin™ for integrin $\alpha_v\beta_3$ and high expression level of integrin $\alpha_v\beta_3$ on the U87MG cell surface.

Immunoreactivity and Binding Specificity

The immunoreactivity of DOTA–Abegrin™ was compared with Abegrin™ by competition binding assay using ^{125}I-Abegrin™ as a radioligand. As shown in Fig. 1c, no obvious difference was observed between the DOTA–Abegrin™ and Abegrin™, indicating that DOTA conjugation had minimal effect on the immunoreactivity of Abegrin™.

The binding of ^{111}In-DOTA–Abegrin™ to U87MG cells can be significantly inhibited by adding an excess dose of Abegrin™, demonstrating the *in vitro* specific binding of ^{111}In-DOTA–Abegrin™ to integrin $\alpha_v\beta_3$ on U87MG cells (Fig. 1d).

Integrin $\alpha_v\beta_3$ Expression on Tumor Cells

The expression of integrin $\alpha_v\beta_3$ on U87MG and HT-29 cells was detected by fluorescent staining and radioligand binding assay. As shown in Fig. 2a, Abegrin™ bound strongly to U87MG cells but not HT-29 cells. Prominently, the specific staining of Abegrin™ was observed mostly on the cell membrane as integrin $\alpha_v\beta_3$ is mainly expressed on the cell surface. The binding fraction of ^{125}I-Abegrin™ on U87MG was about 30%AD/10^6 cells, and the cell-bound ^{125}I-Abegrin™ was significantly blocked by adding an excess dose of cold Abegrin™, indicating the specific binding of ^{125}I-Abegrin™ on U87MG cells (Fig. 2b). In contrast, HT-29 cells can bind ^{125}I-Abegrin™ only at an extremely low level, which was consistent with the result shown in Fig. 2a. Overall, integrin $\alpha_v\beta_3$ is highly expressed on U87MG cells but lowly or nonexpressed on HT-29 cells.

Immunofluorescence Staining of U87MG and HT-29 Tumor Tissues

U87MG and HT-29 frozen tumor sections were stained for human integrin $\alpha_v\beta_3$ and mouse integrin $\alpha_v\beta_3$. As shown in Fig. 2c, U87MG tumors were found to be positive for human integrin $\alpha_v\beta_3$, while HT-29 tumors did not express human integrin $\alpha_v\beta_3$, which was consistent with the above cell results. Both U87MG and HT-29 tumor tissues expressed murine integrin $\alpha_v\beta_3$ due to the generation of newborn tumor blood vessels in the xenografted tumors. There was no colocalization between Abegrin™ staining and murine integrin $\alpha_v\beta_3$ for U87MG tumors because Abegrin™ recognizes only the human tumor cells, but not the mouse tumor vasculature.

Planar γ Imaging

The representative planar γ images acquired at several time points after injection of ^{111}In-DOTA–Abegrin™ are shown in Fig. 3a. Note that although both posterior and anterior images could be acquired simultaneously by the two-headed camera, we only showed the representative posterior images here because they were closer to the mice and had less blurred images than the anterior images. At 2 h post-injection, radioactivity was mainly accumulated in the heart and abdomen. The U87MG (right) and HT-29 (left) tumors were gradually visualized from 24 h postinjection. With the clearance of the radiotracer from normal organs, the tumor visualization was clearer, and the activity accumulation in U87MG tumors was higher than that in HT-29 tumors. At 120 h postinjection, the U87MG tumors showed high contrast of activity accumulation, which was significantly higher than that of HT-29 tumors. Liver is also visible due to the liver clearance of ^{111}In-DOTA–Abegrin™.

In Vivo Microdistribution of FITC–Abegrin™ in Tumors

To investigate the in vivo microdistribution of Abegrin™ in tumors, we labeled Abegrin™ with FITC. FITC–Abegrin™ was injected into nude mouse bearing both U87MG and HT-29 tumors, and the mouse was sacrificed at 24 h postinjection. The tumors and normal organs slices were costained with CD31. We performed the *in vivo* micro-distribution study at 24 h

p.i. because the tumor uptake of Abegrin™ at 24 h p.i. could reach a high level (similar to that at 72 h p.i., see below the *ex vivo* biodistribution data). Most importantly, we believe that the *in vivo* stability of FITC–Abegrin™ at 24 h p.i. was much better than that at 72 h p.i. so that the fluorescent signal determined by microdistribution study may truly reflect the Abegrin™ location in tumors. As shown in Fig. 3b, both U87MG and HT-29 tumors showed predominant CD31 positive staining, indicating the high density of tumor vasculature in both of two tumors. The distribution of FITC–Abegrin™ in HT-29 tumor was almost localized around the tumor vasculature as determined by the good overlay of FITC with CD31. In contrast, besides the localization around the blood vessels, FITC–Abegrin™ also showed predominant tumor cell staining on U87MG tumors, indicating that FITC–Abegrin™ could bind to the U87MG tumor cells *in vivo*.

Biodistribution Studies

Biodistribution of ^{111}In-DOTA–Abegrin™ was determined in nude mice bearing U87MG tumors, and the results are shown in Fig. 4a. The uptake of ^{111}In-DOTA–Abegrin™ in U87MG tumors increased steadily from 4 h to 72 h p.i and then decreased from 72 h to 168 h p.i.(tumor uptake value was 6.19±1.16, 14.12±0.44, 14.85±4.73, 11.47±3.51, and 11.40±0.07%ID/g at 4, 24, 72, 120, and 168 h, respectively). Radioactivity levels of ^{111}In-DOTA–Abegrin™ in blood were 31.31±7.16%ID/g at 4 h p.i, followed by a rather rapid clearance by the end of 168 h (1.17±1.02%ID/g). ^{111}In-DOTA–Abegrin™ also showed predominant liver and spleen uptake, while the kidney uptake was relatively low. At 72 h p.i, the uptake of ^{111}In-DOTA–Abegrin™ was 14.21±1.47%ID/g for liver, 11.35±2.51%ID/g for spleen, and 2.29±0.71%ID/g for kidney, respectively. The bone uptake of ^{111}In-DOTA–Abegrin™ was very low (less than 1%ID/g at any time point), indicating the in vivo stability of the tracer. With the clearance of ^{111}In-DOTA–Abegrin™ from blood and normal organs, the radioactive ratios of tumor to nontumor increased with time. At 168 h p.i, the ratios were 53.10±15.31 for blood, 1.45±0.24 for liver, 2.13±1.05 for kidney, 11.21±6.30 for muscle, and 49.57±14.75 for bone, respectively.

The tumor-targeting specificity of ^{111}In-DOTA–Abegrin™ was detected by blocking study. The coinjection of an excess dose of cold Abegrin™ with ^{111}In-DOTA–Abegrin™ resulted in a significantly reduced tumor uptake at 24 h p.i. (from 14.12±0.44 to 6.93±0.94%ID/g, n=4, PG0.01), indicating that the radioactivity uptake in U87MG tumors was at least partially integrin $\alpha_v\beta_3$-mediated. The cold Abegrin™ did not totally block the tumor uptake of ^{111}In-DOTA–Abegrin™, which might be caused by the nonspecific targeting of large molecules, e.g., enhanced permeability and retention (EPR) effect [31]. The blocking study did not significantly affect the radioactivity uptake in other normal organs, such as heart, liver, and spleen, demonstrating that ^{111}In-DOTA–Abegrin™ did not specifically target the normal organs. The blood uptake also decreased after blocking, which might result from the enhanced blood clearance of ^{111}In-DOTA–Abegrin™ when coinjected with an excess dose of Abegrin™ (Fig. 4b).

Discussion

In the present study, the *in vitro* and *in vivo* integrin $\alpha_v\beta_3$ targeting properties of Abegrin™, a fully humanized monoclonal antibody against integrin $\alpha_v\beta_3$, was investigated, and the ^{111}In-labeled Abegrin™ (^{111}In-DOTA–Abegrin™) was evaluated as a SPECT tracer for molecular imaging of integrin $\alpha_v\beta_3$ expression.

Recently, Cai *et al*. investigated the effect of DOTA conjugation with different DOTA/Abegrin™ reaction ratios (20:1, 50:1, 100:1, 200:1, and 1,000:1) on the tumor uptake of the resulting ^{64}Cu-labeled Abegrin™ [21]. The result showed that the ratio of 200:1 was enough for the conjugation and radiolabeling. We conjugated Abegrin™ with DOTA at a reaction ratio of 200:1 for ^{111}In labeling, and the result revealed that the conjugation of DOTA under this condition did not impair the integrin $\alpha_v\beta_3$ binding specificity and affinity of Abegrin™ (Fig. 1c). It has been well documented for the relatively low *in vivo* thermodynamic and kinetic stability of ^{64}Cu-DOTA [32–34]. The instability of the ^{64}Cu-DOTA conjugates would result in demetallization and subsequent accumulation in nontarget tissues such as liver [35]. Compared with ^{64}Cu-DOTA–Abegrin™, the liver uptake of ^{111}In-DOTA–Abegrin™ was significantly reduced, possibly because the DOTA-chelating ability for ^{111}In is much stronger than that for ^{64}Cu.

Integrin $\alpha_v\beta_3$ is highly expressed not only on some tumor cells but also on the activated endothelial cells of the newborn blood vessels [7, 36]. U87MG (human integrin $\alpha_v\beta_3$-positive) and HT-29 (human integrin $\alpha_v\beta_3$-negative) tumor cells were inoculated into nude mice; therefore, the two tumor tissues both expressed murine integrin $\alpha_v\beta_3$ on the tumor neovasculature (Fig. 2c). Abegrin™ cross-reacts with integrin $\alpha_v\beta_3$ originated from rabbit, chicken, and hamster, but not from mouse [21] so Abegrin™ can recognize only the human integrin $\alpha_v\beta_3$ on the tumor cells but not the murine integrin $\alpha_v\beta_3$ on the tumor vasculature. In the human integrin $\alpha_v\beta_3$-negative HT-29 tumors, FITC–Abegrin™ almost accumulated around the tumor vasculature (Fig. 3b), which was most likely due to the nonspecific targeting of EPR (enhanced permeability and retention [31, 37]) effect of tumors, instead of specific tumor vasculature targeting. In the human integrin $\alpha_v\beta_3$-positive U87MG tumors, besides the specific targeting of Abegrin™ to the tumor cells, a large amount of antibody molecules also remained untargeted to the vasculature (Fig. 3b), indicating that the accumulation of Abegrin™ in integrin $\alpha_v\beta_3$-positive tumors was caused by both specific and nonspecific targeting.

Comparing with radiolabeled RGD tracers, ^{111}In-labeled anti-integrin $\alpha_v\beta_3$ antibody exhibited a quite different pharmacokinetics, such as the slower blood clearance, higher liver and spleen uptake, and high passive tumor targeting. The high nonspecific targeting of Abegrin™ in tumors reminds that caution should be taken when using ^{111}In-DOTA–Abegrin™ as a noninvasive imaging agent to directly quantify the integrin $\alpha_v\beta_3$ expression level *in vivo*. Aerts et al. recently found a disparity between the tumor uptake of ^{89}Zr-labeled anti-EGFR antibody cetuximab and *in vivo* EGFR expression on tumors [38], which may be due to the complex microenvironment of tumors (e.g., inadequate vasculature and perfusion). In another report [39], the tumor uptake of ^{111}In-labeled anti-HER2 antibody trastuzumab showed much stronger, nonlinear associations with HER2 density if it was

corrected for nonspecific IgG localization ($r^2 = 0.99$), but without the correction, the association between HER2 density and tumor uptake was poor ($r^2 = 0.22$). Therefore, further study using ^{111}In-labeled IgG or HSA as the nonspecific imaging agents to quantify the nonspecific uptake values in different tumor models may be helpful for quantitatively measuring the specific targeting values of ^{111}In-DOTA–Abegrin™, which would provide more information on the receptor expression levels.

It also should be noted that the *in vivo* targeting property of ^{111}In-DOTA–Abegrin™ in the present study may not truly reflect the clinical situation because Abegrin™ does not bind the murine integrin $\alpha_v\beta_3$ expressed on tumor new-bone vasculatures of mice. In human, Abegrin™ would bind both integrin $\alpha_v\beta_3$-positive tumor cells and the activated endothelial cells in tumor blood vessels. The high human integrin $\alpha_v\beta_3$ binding affinity and specificity of ^{111}In-DOTA–Abegrin™ as demonstrated in this study guarantee that ^{111}In-DOTA–Abegrin™ is promising for both integrin $\alpha_v\beta_3$-positive tumors imaging and tumor angiogenesis imaging in clinic.

In conclusion, ^{111}In-labeled Abegrin™ exhibited high *in vitro* specificity and immunoreactivity against integrin $\alpha_v\beta_3$ on tumor cells. Due to the specific receptor targeting, the *in vivo* uptake of ^{111}In-DOTA–Abegrin™ in integrin $\alpha_v\beta_3$-positive tumors was significantly higher than that in integrin $\alpha_v\beta_3$-negative tumors. The human integrin $\alpha_v\beta_3$-specific targeting of ^{111}In-DOTA–Abegrin™ may be translated to clinic for noninvasive measurement of integrin $\alpha_v\beta_3$ in the tumors and also providing essential information in the evaluation of Abegrin™-based antiangiogenic therapy, as well as ^{90}Y-Abegrin™-based radioimmunotherapy.

Acknowledgments

We thank Mr. Zhi Yang and Mr. Cunjing Jin for their excellent technical assistance with γ-imaging and biodistribution studies. This work is jointly supported by NSFC projects (30930030, 30870728, 30900373, and 20820102035), an 863 project (2007AA02Z467), and grants from the Ministry of Science and Technology of China (2009ZX09103-733, 2009ZX09301-010, and 2009ZX09103-746).

References

1. Eble JA, Haier J. Integrins in cancer treatment. Curr Cancer Drug Targets. 2006; 6:89–105. [PubMed: 16529540]
2. Giancotti FG, Ruoslahti E. Integrin signaling. Science. 1999; 285:1028. [PubMed: 10446041]
3. Hynes RO. Integrins: versatility, modulation, and signaling in cell adhesion. Cell. 1992; 69:11–25. [PubMed: 1555235]
4. Seftor RE, Seftor EA, Gehlsen KR, Stetler-Stevenson WG, Brown PD, Ruoslahti E, Hendrix MJ. Role of the alpha v beta 3 integrin in human melanoma cell invasion. Proc Natl Acad Sci U S A. 1992; 89:1557–1561. [PubMed: 1371877]
5. Eliceiri BP, Cheresh DA. The role of alphav integrins during angiogenesis: insights into potential mechanisms of action and clinical development. J Clin Invest. 1999; 103:1227–1230. [PubMed: 10225964]
6. Kumar CC. Integrin alpha v beta 3 as a therapeutic target for blocking tumor-induced angiogenesis. Curr Drug Targets. 2003; 4:123–131. [PubMed: 12558065]
7. Brooks PC, Clark RA, Cheresh DA. Requirement of vascular integrin alpha v beta 3 for angiogenesis. Science. 1994; 264:569–571. [PubMed: 7512751]

8. Veeravagu A, Liu Z, Niu G, Chen K, Jia B, Cai W, Jin C, Hsu AR, Connolly AJ, Tse V, et al. Integrin alphavbeta3-targeted radioimmunotherapy of glioblastoma multiforme. Clin Cancer Res. 2008; 14:7330–7339. [PubMed: 19010848]
9. Shi J, Jia B, Liu Z, Yang Z, Yu Z, Chen K, Chen X, Liu S, Wang F. 99mTc-labeled bombesin(7–14)NH2 with favorable properties for SPECT imaging of colon cancer. Bioconjug Chem. 2008; 19:1170–1178. [PubMed: 18491928]
10. Liu Z, Wang F, Chen X. Integrin alpha v beta 3-targeted cancer therapy. Drug Development Research. 2008; 69:329–339. [PubMed: 20628538]
11. Beer AJ, Grosu AL, Carlsen J, Kolk A, Sarbia M, Stangier I, Watzlowik P, Wester HJ, Haubner R, Schwaiger M. [18F]galacto-RGD positron emission tomography for imaging of alphavbeta3 expression on the neovasculature in patients with squamous cell carcinoma of the head and neck. Clin Cancer Res. 2007; 13:6610–6616. [PubMed: 18006761]
12. Beer AJ, Haubner R, Wolf I, Goebel M, Luderschmidt S, Niemeyer M, Grosu AL, Martinez MJ, Wester HJ, Weber WA, et al. PET-based human dosimetry of 18F–galacto-RGD, a new radiotracer for imaging alpha v beta3 expression. J Nucl Med. 2006; 47:763–769. [PubMed: 16644745]
13. Morrison MS, Ricketts SA, Barnett J, Cuthbertson A, Tessier J, Wedge SR. Use of a novel Arg-Gly-Asp radioligand, 18F–AH111585, to determine changes in tumor vascularity after antitumor therapy. J Nucl Med. 2009; 50:116–122. [PubMed: 19091899]
14. Liu Z, Niu G, Shi J, Liu S, Wang F, Liu S, Chen X. (68)Ga-labeled cyclic RGD dimers with Gly(3) and PEG (4) linkers: promising agents for tumor integrin alpha (v)beta (3) PET imaging. Eur J Nucl Med Mol Imaging. 2009; 36:947–957. [PubMed: 19159928]
15. Tucker GC. Integrins: molecular targets in cancer therapy. Curr Oncol Rep. 2006; 8:96–103. [PubMed: 16507218]
16. Gutheil JC, Campbell TN, Pierce PR, Watkins JD, Huse WD, Bodkin DJ, Cheresh DA. Targeted antiangiogenic therapy for cancer using Vitaxin: a humanized monoclonal antibody to the integrin alphavbeta3. Clin Cancer Res. 2000; 6:3056–3061. [PubMed: 10955784]
17. Wu H, Beuerlein G, Nie Y, Smith H, Lee BA, Hensler M, Huse WD, Watkins JD. Stepwise *in vitro* affinity maturation of Vitaxin, an alphav beta3-specific humanized mAb. Proc Natl Acad Sci USA. 1998; 95:6037. [PubMed: 9600913]
18. Cai W, Chen X. Anti-angiogenic cancer therapy based on integrin alphavbeta3 antagonism. Anticancer Agents Med Chem. 2006; 6:407–428. [PubMed: 17017851]
19. Delbaldo C, Raymond E, Vera K, Hammershaimb L, Kaucic K, Lozahic S, Marty M, Faivre S. Phase I and pharmacokinetic study of etaracizumab (Abegrin), a humanized monoclonal antibody against alphavbeta3 integrin receptor, in patients with advanced solid tumors. Invest New Drugs. 2008; 26:35–43. [PubMed: 17876527]
20. Posey JA, Khazaeli MB, DelGrosso A, Saleh MN, Lin CY, Huse W, LoBuglio AF. A pilot trial of Vitaxin, a humanized anti-vitronectin receptor (anti alpha v beta 3) antibody in patients with metastatic cancer. Cancer Biother Radiopharm. 2001; 16:125–132. [PubMed: 11385959]
21. Cai W, Wu Y, Chen K, Cao Q, Tice DA, Chen X. *In vitro* and *in vivo* characterization of 64Cu-labeled Abegrin, a humanized monoclonal antibody against integrin alpha v beta 3. Cancer Res. 2006; 66:9673–9681. [PubMed: 17018625]
22. Scheer MG, Stollman TH, Boerman OC, Verrijp K, Sweep FC, Leenders WP, Ruers TJ, Oyen WJ. Imaging liver metastases of colorectal cancer patients with radiolabelled bevacizumab: Lack of correlation with VEGF-A expression. Eur J Cancer. 2008; 44:1835–1840. [PubMed: 18632262]
23. Iagaru A, Gambhir SS, Goris ML. 90Y–ibritumomab therapy in refractory non-Hodgkin's lymphoma: observations from 111In-ibritu-momab pretreatment imaging. J Nucl Med. 2008; 49:1809–1812. [PubMed: 18927323]
24. Pandit-Taskar N, O'Donoghue JA, Morris MJ, Wills EA, Schwartz LH, Gonen M, Scher HI, Larson SM, Divgi CR. Antibody mass escalation study in patients with castration-resistant prostate cancer using 111In-J591: lesion detectability and dosimetric projections for 90Y radioimmunotherapy. J Nucl Med. 2008; 49:1066–1074. [PubMed: 18552139]
25. Behr TM, Behe M, Wormann B. Trastuzumab and breast cancer. N Engl J Med. 2001; 345:995–996. [PubMed: 11575295]

26. Banning A, Kipp A, Schmitmeier S, Lowinger M, Florian S, Krehl S, Thalmann S, Thierbach R, Steinberg P, Brigelius-Flohe R. Glutathione Peroxidase 2 Inhibits Cyclooxygenase-2-Mediated Migration and Invasion of HT-29 Adenocarcinoma Cells but Supports Their Growth as Tumors in Nude Mice. Cancer Res. 2008; 68:9746–9753. [PubMed: 19047153]
27. Liu Z, Yu Z, He W, Ma S, Sun L, Wang F. *In-vitro* internalization and *in-vivo* tumor uptake of anti-EGFR monoclonal antibody LA22 in A549 lung cancer cells and animal model. Cancer Biother Radiopharm. 2009; 24:15–24. [PubMed: 19216631]
28. Shao W, Zhao S, Liu Z, Zhang J, Ma S, Sato JD, Zhang P, Tong M, Han J, Wang Y, et al. Inhibition of human tumor xenograft growth in nude mice by a conjugate of monoclonal antibody LA22 to epidermal growth factor receptor with anti-tumor antibiotics mitomycin C. Biochem Biophys Res Commun. 2006; 349:816–824. [PubMed: 16950201]
29. Liu Z, Yan Y, Chin FT, Wang F, Chen X. Dual Integrin and Gastrin-Releasing Peptide Receptor Targeted Tumor Imaging Using (18)F-labeled PEGylated RGD-Bombesin Heterodimer (18)F-FB-PEG (3)-Glu-RGD-BBN. J Med Chem. 2009; 52:425–432. [PubMed: 19113865]
30. He Q, Liu Z, Jia B, Li X, Shi J, Zhang J, Lan F, Yang Z, Liu Y, Shen L, et al. *In vivo* gamma imaging of the secondary tumors of transplanted human fetal striatum neural stem cells-derived primary tumor cells. Neuroreport. 2008; 19:1009–1014. [PubMed: 18580570]
31. Maeda H, Fang J, Inutsuka T, Kitamoto Y. Vascular permeability enhancement in solid tumor: various factors, mechanisms involved and its implications. Int Immunopharmacol. 2003; 3:319–328. [PubMed: 12639809]
32. Boswell CA, Sun X, Niu W, Weisman GR, Wong EH, Rheingold AL, Anderson CJ. Comparative *in vivo* stability of copper-64-labeled cross-bridged and conventional tetraazamacrocyclic complexes. J Med Chem. 2004; 47:1465–1474. [PubMed: 14998334]
33. Liu Z, Li Z, Cao Q, Liu S, Wang F, Chen X. Small-Animal PET of Tumors with 64Cu-Labeled RGD-Bombesin Heterodimer. J Nucl Med. 2009; 50:1168–1177. [PubMed: 19525469]
34. Sprague JE, Peng Y, Sun X, Weisman GR, Wong EH, Achilefu S, Anderson CJ. Preparation and biological evaluation of copper-64-labeled tyr3-octreotate using a cross-bridged macrocyclic chelator. Clin Cancer Res. 2004; 10:8674–8682. [PubMed: 15623652]
35. Prasanphanich AF, Nanda PK, Rold TL, Ma L, Lewis MR, Garrison JC, Hoffman TJ, Sieckman GL, Figueroa SD, Smith CJ. [64Cu-NOTA-8-Aoc-BBN(7–14)NH2] targeting vector for positron-emission tomography imaging of gastrin-releasing peptide receptor-expressing tissues. Proc Natl Acad Sci U S A. 2007; 104:12462–12467. [PubMed: 17626788]
36. Gladson CL. Expression of integrin alpha v beta 3 in small blood vessels of glioblastoma tumors. J Neuropathol Exp Neurol. 1996; 55:1143–1149. [PubMed: 8939197]
37. Maeda H. The enhanced permeability and retention (EPR) effect in tumor vasculature: the key role of tumor-selective macromolecular drug targeting. Adv Enzyme Regul. 2001; 41:189–207. [PubMed: 11384745]
38. Aerts HJ, Dubois L, Perk L, Vermaelen P, van Dongen GA, Wouters BG, Lambin P. Disparity between *in vivo* EGFR expression and 89Zr-labeled cetuximab uptake assessed with PET. J Nucl Med. 2009; 50:123–131. [PubMed: 19091906]
39. McLarty K, Cornelissen B, Scollard DA, Done SJ, Chun K, Reilly RM. Associations between the uptake of 111In-DTPA-trastuzumab, HER2 density and response to trastuzumab (Herceptin) in athymic mice bearing subcutaneous human tumour xenografts. Eur J Nucl Med Mol Imaging. 2009; 36:81–93. [PubMed: 18712381]

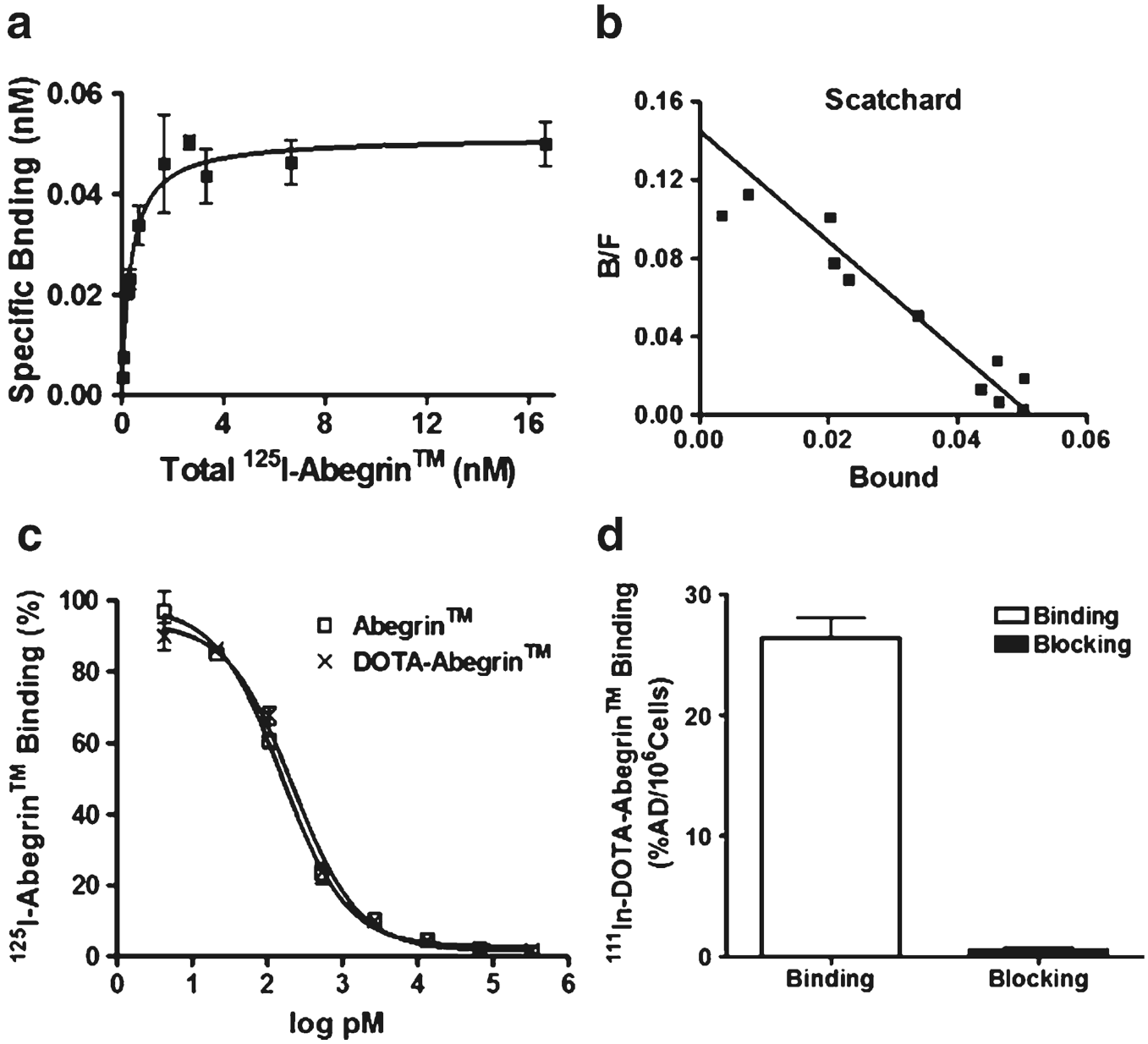

Fig. 1.

Saturation binding curve (**a**) and Scatchard transformation (**b**) of ^{111}In-DOTA–Abegrin™ to U87MG cells; **c** the binding of ^{125}I-Abegrin™ to U87MG cells in the presence of increasing concentrations of DOTA–Abegrin™ or Abegrin™; **d** Binding of ^{111}In-DOTA–Abegrin™ to U87MG cells with or without an excess dose of cold Abegrin™. Each data point represents the mean±SD of triplicate measurements.

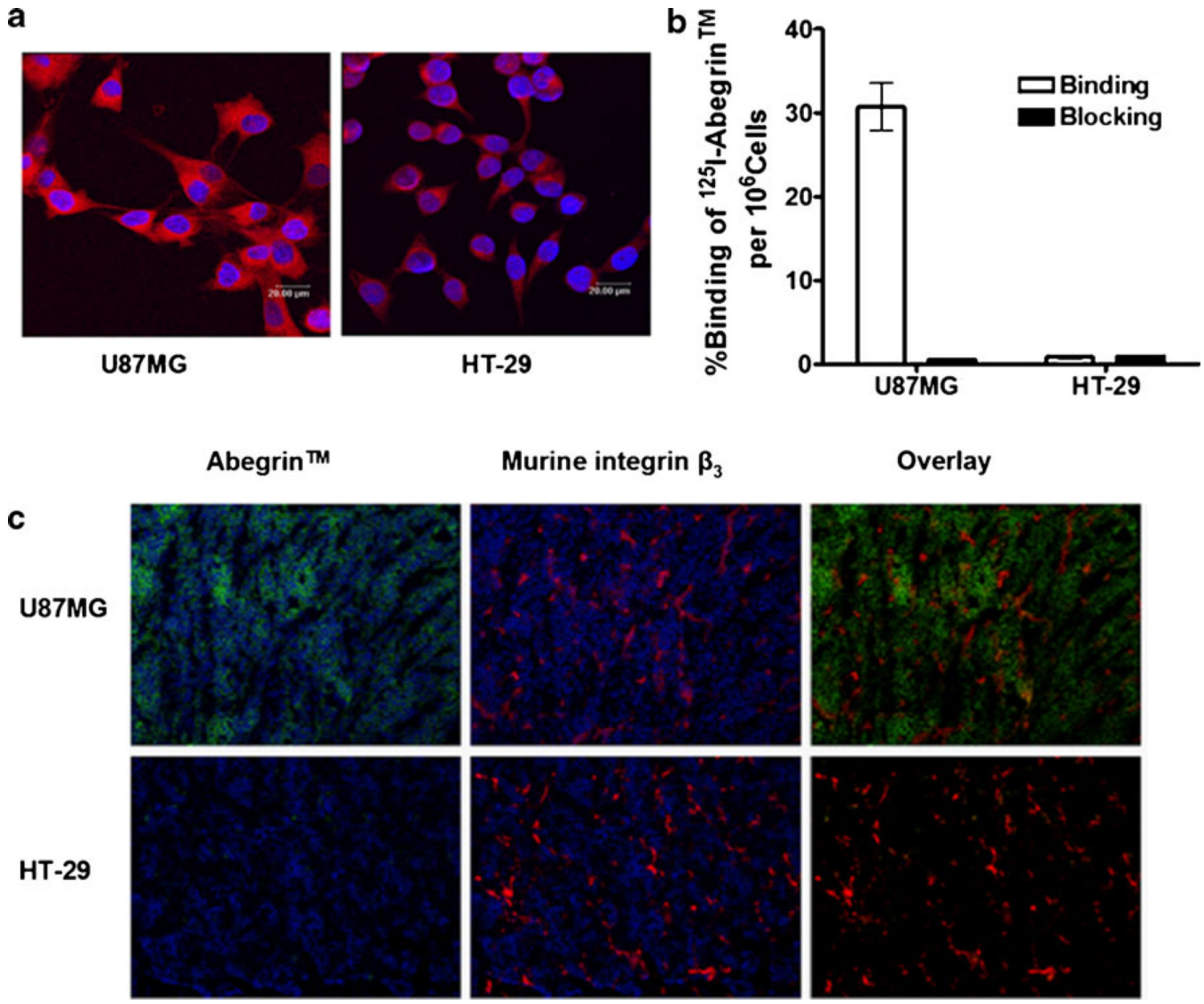

Fig. 2.

a Immunofluorescence staining of U87MG and HT-29 cells using Abegrin™ as the primary antibody; **b** Binding of ^{125}I-Abegrin™ to U87MG or HT-29 cells with or without an excess dose of cold Abegrin™ (n=3, bars represent means±SD); **c** human integrin $\alpha_v\beta_3$ (Abegrin™ as the primary antibody) and mouse integrin β_3 staining of U87MG and HT-29 tumor sections.

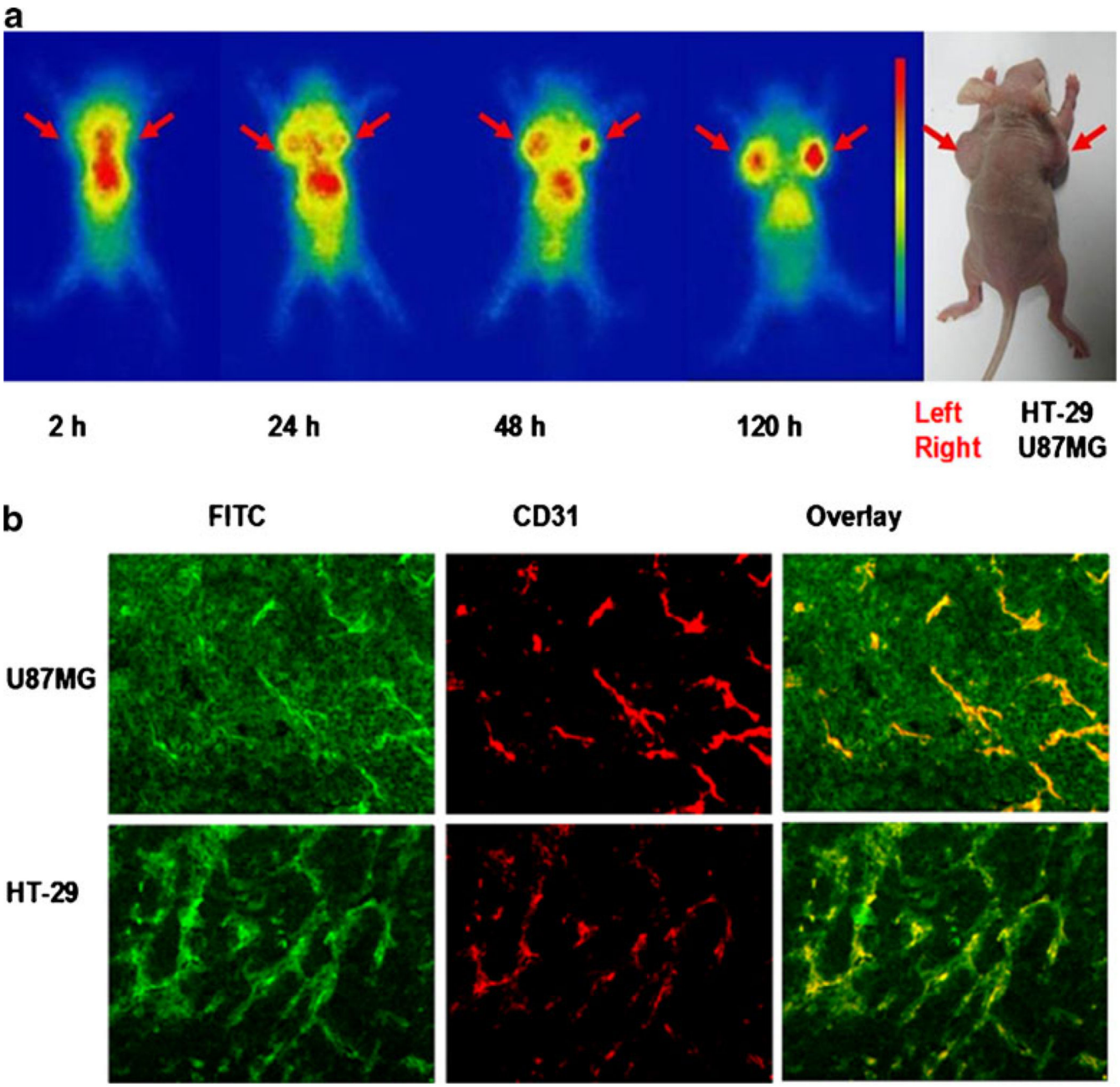

Fig. 3.

a Nude mice bearing both U87MG and HT-29 tumor xenografts were injected intravenously with ~300 μCi of ^{111}In-DOTA–Abegrin™, and then planar γ images were acquired at 2, 24, 48, and 120 h postinjection. *Arrows* indicate the tumor location; **b** FITC–Abegrin™ was injected intravenously into nude mice bearing both U87MG and HT-29 tumor xenografts. At 24 h postinjection, the tumors were cut into slices and then stained with antimouse CD31 antibody.

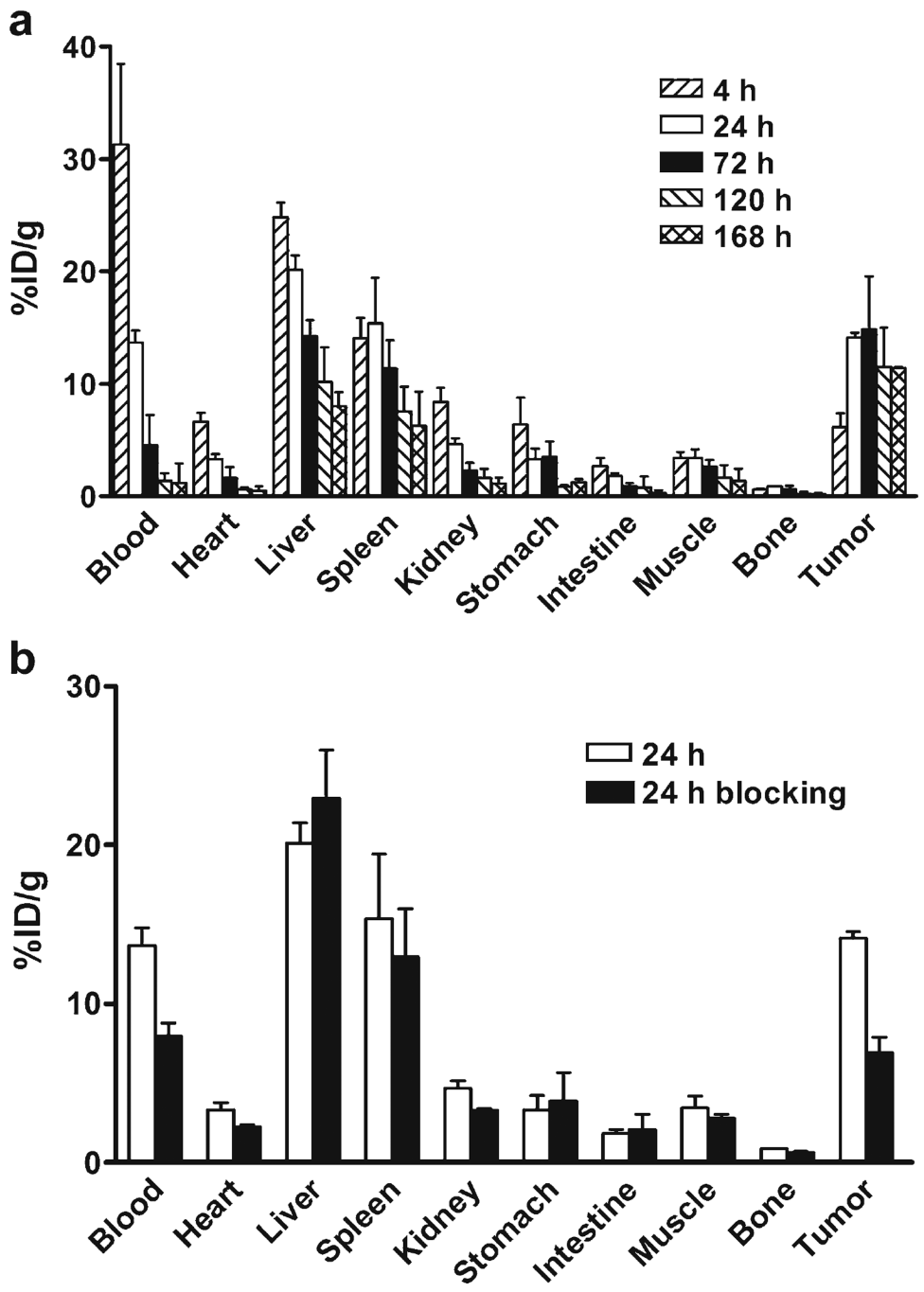

Fig. 4.

a Biodistribution of ^{111}In-DOTA–Abegrin™ in U87MG tumor-bearing nude mice at 4, 24, 72, 120, and 168 h post-injection; **b** biodistribution of ^{111}In-DOTA–Abegrin™ in U87MG tumor-bearing nude mice with and without coinjection of an excess dose of cold Abegrin™ as a blocking agent at 24 h postinjection. Data are expressed as %ID/g±SD (n=4 per group).